Physics Letters A 380 (2016) 83–87

Contents lists available at ScienceDirect

Physics Letters A

www.elsevier.com/locate/pla

Two-dimensional capillary origami

N.D. Brubaker *, J. Lega

Department of Mathematics, University of Arizona, Tucson, AZ, 85721, USA

ARTICLE INFO

Article history:
Received 9 July 2015
Received in revised form 1 September 2015
Accepted 2 September 2015
Available online 8 September 2015
Communicated by C.R. Doering

Keywords:
Elasto-capillary system
Capillary origami
Nonlinear plate
Energy minimization

ABSTRACT

We describe a global approach to the problem of capillary origami that captures all unfolded equilibrium configurations in the two-dimensional setting where the drop is not required to fully wet the flexible plate. We provide bifurcation diagrams showing the level of encapsulation of each equilibrium configuration as a function of the volume of liquid that it contains, as well as plots representing the energy of each equilibrium branch. These diagrams indicate at what volume level the liquid drop ceases to be attached to the endpoints of the plate, which depends on the value of the contact angle. As in the case of pinned contact points, three different parameter regimes are identified, one of which predicts instantaneous encapsulation for small initial volumes of liquid.

1. Introduction

Capillary origami, namely the folding of a flexible two-dimensional membrane into a predetermined three-dimensional shape through the action of surface capillary forces, is an example of micro-origami [1]. This technique (see [2] for a review), which also encompasses folding of planar structures by means of chemical [3], thermal [4], and electrostatic forces [5,6], presents an interesting alternative to the traditional methods of micro-fabrication based on the deposition and etching of thin films [7,8]. Capillary origami is observed in nature [9] and its applications include lab-on-a-chip devices [10], graphene actuation [11] and self-assembly [12–14].

The seminal article of Py et al. [15] provided an elegant proof of concept for capillary origami, showing that a variety of three-dimensional structures, such as cubes or pyramids, could be created by this method. A capillary origami system consists of a thin, flat two-dimensional plate, lying on a hydrophobic substrate, over which one places a small drop of liquid. Initially, the solid–liquid adhesive forces overcome the strength of elastic forces within the plate, deforming the system into an equilibrium position where the plate at least partially adheres to the drop of liquid. As the volume of liquid is reduced, for instance by evaporation [16–19], the thin sheet can completely encapsulate the liquid, thereby forming a three-dimensional structure whose shape is predetermined by the initial cut out of the two-dimensional thin film. Alternatively, immediate folding may be achieved upon impact of a drop on a flexible membrane [20].

The purpose of this letter is to promote a unified and systematic approach to the problem of capillary origami and to apply this method to identify all two-dimensional equilibrium structures of a capillary origami system in the general situation where the liquid is not required to completely wet the flexible plate. The shape of the air–liquid interface, as well as the extent over which the liquid is in contact with the plate, are obtained as consequences of minimizing the total energy E of the system, under appropriate constraints. This minimization is performed on the actual energy, as opposed to for instance a discretized version thereof [18]. As a consequence, we obtain the ordinary differential equations and boundary conditions that equilibria must satisfy. These are Equations (2), which we then solve numerically, using an Euler–Newton predictor–corrector method. The resulting equilibrium configurations depend on the physical properties of the fluid and of the plate, as well as on a single control parameter, which is the volume of the liquid.

We present our results in the form of bifurcation diagrams showing the level of encapsulation of various branches of equilibria as a function of the volume V of liquid in the system, together with corresponding plots for E. These plots explain how the bifurcation diagrams of [21], obtained for configurations in which the liquid wets the entire plate, are amended when partial wetting is taken into account. We conclude that, as in [21] for fixed contact points, *three* parameter regimes need to be considered in the general case.

* Corresponding author.
E-mail addresses: nbrubaker@math.arizona.edu (N.D. Brubaker), lega@math.arizona.edu (J. Lega).

http://dx.doi.org/10.1016/j.physleta.2015.09.002
0375-9601/

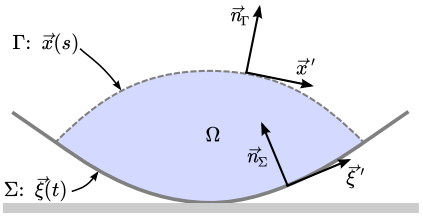

Fig. 1. Two-dimensional capillary origami setup.

2. Problem setup

For simplicity, we neglect gravity and assume that the plate bends without stretching. These effects, as well as the presence of external forces generated for instance by an electric [22] or magnetic [23] field, may be included in the total energy of the system if needed. We suppose that all deformations are elastic, and we are only concerned with two-dimensional structures, that is three-dimensional configurations that are uniform by translation in one spatial direction. We therefore consider the two-dimensional capillary origami setup shown in Fig. 1, consisting of a thin plate Σ and a drop of liquid Ω whose interface with the surrounding air is given by the curve Γ. The volume V of the drop of liquid (denoted as the area A of the region delimited by Γ and Σ), as well as the length L of the plate, are fixed and finite. We look for configurations that are symmetric with respect to the vertical axis, but do not assume any particular shape for Γ or Σ. These properties will be obtained as consequences of the minimization process.

To streamline the discussion, we explain our approach in the situation where the endpoints of Γ and Σ are in contact but give the final result in (2) for general configurations; an example of the latter is depicted in Fig. 1. Details of the calculations are given in [21] for pinned contact points and summarized in the supplementary materials for non-pinned contact points. A longer article describing the calculations in the latter case is in progress and will be published elsewhere [24].

When the fluid wets the entire plate, the total energy of the system is comprised of the free surface energy of the liquid–air interface [25], and of the bending energy of the elastic plate [26]. This energy is given by $\gamma\, L\, E[\Gamma,\Sigma]$, where $\gamma \equiv \gamma_{LV}$ is the surface tension of the liquid–vapor interface Γ and $E[\Gamma,\Sigma]$ is the dimensionless energy

$$E[\Gamma,\Sigma] = \int_\Gamma d\sigma + \frac{1}{2\lambda}\int_\Sigma {\kappa_\Sigma}^2 d\sigma. \tag{1}$$

The elasto-capillary length of the system is given by $L_{ec} = L/\sqrt{\lambda}$ where $\lambda = \gamma L^2/B$ and B is the bending rigidity of Σ. In (1), all lengths are relative to the length L of the plate, κ denotes the signed curvature of its subscript, and $d\sigma$ represents the arc-length element of the curve referred to in each integral. As detailed in [21], equilibrium configurations are obtained by calculating the first variation of the above energy assuming conservation of the volume of liquid V and the length of the plate L. Using α and β as Lagrange multipliers to account for these constraints, one must therefore minimize

$$\mathcal{J}[\Gamma,\Sigma] = \int_\Gamma d\sigma + \frac{1}{2\lambda}\int_\Sigma {\kappa_\Sigma}^2 d\sigma + \alpha\int_\Sigma d\sigma + \beta\iint_\Omega dA.$$

To this end, we introduce perturbations Γ_ϵ and Σ_ϵ of the curves Γ and Σ parametrized as follows:

$$\Gamma_\epsilon: \quad \vec{x}_\epsilon(s) = \vec{x}(s) + \epsilon\left(u_\Gamma(s)\,\vec{n}_\Gamma(s) + v_\Gamma(s)\,\vec{x}'(s)\right),$$
$$\Sigma_\epsilon: \quad \vec{\xi}_\epsilon(t) = \vec{\xi}(t) + \epsilon(u_\Sigma(t)\,\vec{n}_\Sigma(t) + v_\Sigma(t)\,\vec{\xi}'(t)),$$

where $\vec{x}(s) = (x(s), y(s))$ is a smooth parametrization of Γ in terms of its arclength $s \in [-\ell, \ell]$ (here ℓ is the half-length of the air–liquid interface scaled to the length L of the plate), $\vec{\xi}(t) = (\xi(t), \eta(t))$ is a similar parametrization of the plate by its arclength $t \in [-1/2, 1/2]$, a prime represents the derivative with respect to arclength, $\vec{n}_\Gamma(s) = R_{\pi/2}\,\vec{x}'(s)$ and $\vec{n}_\Sigma(t) = R_{\pi/2}\,\vec{\xi}'(t)$ are the corresponding unit normals pointing out of and into the liquid respectively, and R_ω is the standard two-dimensional counter-clockwise rotation matrix of angle ω (see Fig. 1). We do not assume that these perturbations are symmetric with respect to the vertical axis. The tangent and normal vectors for the perturbed air–liquid interface are related by the Serret–Frénet formulas

$$\left(\frac{\vec{x}'_\epsilon}{||\vec{x}'_\epsilon||}\right)' = \kappa_{\Gamma_\epsilon}\,\vec{n}_{\Gamma_\epsilon}\,||\vec{x}'_\epsilon||, \qquad \vec{n}'_{\Gamma_\epsilon} = -\kappa_{\Gamma_\epsilon}\vec{x}'_\epsilon;$$

similar relations also hold for the tangent and normal vectors for the perturbed plate. Requiring that the endpoints of Γ_ϵ are the same as the endpoints of Σ_ϵ leads to expressions for the tangential components of the perturbations,

$$v_\Gamma(\pm\ell) = \frac{\vec{\xi}'\cdot\vec{x}'}{\vec{n}_\Gamma\cdot\vec{\xi}'}u_\Gamma + \frac{1}{\vec{n}_\Sigma\cdot\vec{x}'}u_\Sigma\bigg|_{P_\pm},$$
$$v_\Sigma(\pm 1/2) = \frac{1}{\vec{n}_\Gamma\cdot\vec{\xi}'}u_\Gamma + \frac{\vec{x}'\cdot\vec{\xi}'}{\vec{n}_\Sigma\cdot\vec{x}'}u_\Sigma\bigg|_{P_\pm},$$

where $P_\pm$ denotes the points $(s,t) = \pm(\ell, 1/2)$. The equilibrium configurations, which are extrema of $\mathcal{J}[\Gamma,\Sigma]$, are obtained by calculating the derivative of $\mathcal{J}[\Gamma_\epsilon,\Sigma_\epsilon]$ with respect to ϵ at the value $\epsilon = 0$ and demanding that this derivative vanish for all perturbations u_Γ, u_Σ. This leads to the following equations for the curvatures κ_Γ and κ_Σ of Γ and Σ:

$$\kappa_\Gamma = \beta, \quad -\ell < s < \ell$$
$$\kappa_\Sigma'' + \frac{{\kappa_\Sigma}^3}{2} - \alpha\lambda\kappa_\Sigma = \beta\lambda, \quad -\zeta < t < \zeta, \tag{2a}$$

with boundary conditions

$$\kappa_\Sigma = 0, \quad \kappa_\Sigma{}' = \lambda\,\vec{n}_\Sigma\cdot\vec{x}', \quad \vec{\xi}'\cdot\vec{x}' + \alpha = 0 \tag{2b}$$

at the contact points $(s,t) = \pm(\ell,\zeta)$. The parameter ζ is equal to $1/2$ for pinned contact points. As explained in the supplementary material and detailed in [24], the above equations extend to the case of free contact points, for which $0 < \zeta < 1/2$, with the additional constraints $\alpha \geq -\tau$ and $(\alpha+\tau)(2\zeta - 1) = 0$, where τ is the known relative adhesion coefficient $\tau = (\gamma_{SV} - \gamma_{LS})/\gamma$.

System (2a) immediately implies that the air–liquid interface Γ is, as expected, an arc of a circle and, thus, reduces to a single differential equation for κ_Σ. We showed in [21] that in the case of pinned contact points this is equivalent to the model proposed by Py et al. [15], which is also used in [27] in the idealized case of a plate of infinite length. To the best of our knowledge, the above equations are new for non-pinned contact points. Their significance is detailed in the bifurcation diagrams of the next section.

3. Bifurcation diagrams

In this section, we present bifurcation diagrams that describe all basic equilibrium configurations of a two-dimensional capillary origami system. These diagrams, which complete and extend the diagrams of [15] and [21] to the case of non-pinned contact points, are obtained by numerically solving system (2), allowing the parameter ζ to be less than $1/2$, with the appropriate constraints on α and β mentioned above. These diagrams show the distance across the opening of the plate $\xi(1/2) - \xi(-1/2) \equiv 2\,\xi(1/2)$ as a